Fountain Journal of Natural and Applied Sciences 2018; 7(1): 29-41

DOI: 10.53704/fujnas.v7i1.247

A publication of College of Natural and Applied Sciences, Fountain University, Osogbo, Nigeria.
Journalhomepage:www.fountainjournals.com
ISSN:2354-337X(Online),2350-1863(Print)

Comparative Analysis of Theoretical and Empirical Data of Synthetic Cannabinoids

***[1]Abdulsalami, I.O., [1]Adeoye, M.D., [1]Alabi, K.A., [2]Abdulsalami, B.A. and [1]Abolurin, N.O.**

[1]Department of Chemical Sciences, Fountain University, Osogbo, Nigeria.
[2]Department of Mathematical and Computer Sciences, Fountain University, Osogbo, Nigeria.

Abstract

Comparative studies of spectroscopic data of indol-3-carboxylates and indazole-3-carboxylates are reported from theoretical and empirical viewpoints. Structures of indol-3-carboxylates and indazole-3-carboxylates were modeled; quantum chemical method was employed to investigate the spectroscopic (NMR and FT-IR) properties of the structures. The results obtained from the theoretical studies were compared to empirical results obtained for the spectroscopic properties of these compounds and level of agreement (or disagreement) between the results for the two studies are reported. The scope of the study is limited to the modeling, structural, and electronic and spectroscopic analyses of the modeled structures and comparative analysis of the theoretical data with published experimental data. The absorption transitions were calculated from the optimized geometry in the ground state (S_0) using TD-B3LYP/6-31G**. The energy band gaps calculated showed that Naphthalene-1-yl 1–(5-fluoropentyl)-1H-indazole-3-carboxylate (M5) has the lowest band gap energy, which may have a substantial influence on the intramolecular charge transfer and bioactivity of the molecule. The ^{13}C and ^{1}HNMR chemical shifts calculated at ab initio and DFT agreed with the experimental data. DFT/6-311G** has the best correlation with fitting factor 0.9956.Thus the chemical shifts from DFT/6-311G** are very close to the experimental and can be used in the absence of experimental data. The vibrational frequency analyses by DFT/B3LYP method are in reasonable agreement with the experimental values.

Keywords: Density functional theory; Frontier molecular orbitals; Spectroscopic properties; Basis set; Indazole-3-carboxamide; N-1-methoxycarbonylalkyl group

Introduction

In 2014, Shevyrin and co-workers synthetized five illicit new psychoactive substances (NPS), also known as designer drugs, (cannabinoids) with an indazole-3-carboxamide structure bearing an N-1-methoxycarbonylalkyl group. Shafran *et al.* (2014) reported the experimental identification and analytical characteristics of these synthetic cannabinoids as compounds containing very high cannabimimetic activity which has caused mass severe intoxication and deaths (Wilkinson et al., 2015).

They recognized two main trends of appearance of illegal NPS. Most typical, and simple, is the empirical synthesis of structural analogues of known

---

*Corresponding author:+2348054284452
Email address: aiboldip@gmail.com

narcotics, while the other route involves study of the scientific pharmacological literature to reveal potential structures with the desired effect but which are unregulated (Ware *et al.,* 2010).

Cannabinoids are the active components of *Cannabis sativa* and their derivatives. *Cannabis sativa* produces over sixty unique compounds known as cannabinoids (Shafran, *et al.*, 2014). They exert palliative effects in cancer patients by preventing nausea, vomiting and pain and by stimulating appetite and have been shown to inhibit the growth of tumour cells in culture and animal models by modulating key cell-signalling pathways (Naftali *et al.*, 2013). It is one of the most popular recreational drugs; worldwide, an estimated 178 million people aged 15 to 64 years used cannabis at least once in 2012 (Rajal *et al.*, 2015). The characteristics of carboxylates of the compounds studied in this study will serve as tools for analytical chemists involved in identification of the compounds in seizures of illicit psychoactive compounds.

Cannabinoids are compounds with tetrahydrocannabinol (THC) like structures and/or THC-like pharmacological properties. Many compounds with a THC-like structure are present in cannabis, but not all of them have THC-like pharmacological properties. In addition, some natural or synthetic compounds have THC-like pharmacological properties but not THC-like structure (Sun et al., 2015).

Although the pharmacology of most of the cannabinoids is unknown, it is widely accepted that tetrahydrocannabinol (THC) is the most important, owing to its high potency and abundance in cannabis. Medical cannabis (use of cannabis or cannabinoids as medical therapy to treat disease or alleviate symptoms) has shown that cannabinoids can be administered orally, sub-lingually, or topically; they can be smoked, inhaled, mixed with food, or made into tea (Sun *et al.*, 2015). They can be taken in herbal form, extracted naturally from the plant, gained by isomerization of cannabidiol, or manufactured synthetically.Prescribed cannabinoids include dronabinol capsules, nabilone capsules, and the spray nabiximols (oromucosal) (Elli *et al.*, 2009). Ono *et al.*, (2015) have reported the successful applications of cannabinoids like nabilone, dronabinol, nabiximols, levonantradol and also reported is the use of THC for the treatment of nausea and vomiting due to chemotherapy, either singly or in combinations (Eisenberg *et al.*, 2014).

However, the spectroscopic methods used in structural elucidation of these compounds can be time consuming, cumbersome and complicated. Improved of computer technology and the development of efficient computational methods, has made it possible to make detailed quantum-chemical calculations on molecular property such as geometries, charge distributions, thermodynamic data, vibrational frequency, magnetic resonance parameters, and reaction pathways (Stern and Lambert, 2007; Thomas et al., 2014). Among the computational methods, density functional theory (DFT) calculations have been found to provide admirable results that are in agreement with experimental vibrational frequencies of organic compounds (Semire and Adeoye, 2013). DFT has been extensively used for the calculations of chemical shifts for various types of compounds with good accuracy (Jorge *et al.*, 2012; Lundqvist et al., 2006) due to the implementation of nuclear magnetic resonance (NMR) spin-spin coupling constants within the DFT framework (Belendiuk et al., 2015). Therefore, this study also investigated the performance of Hartree Fock and density functional theory (DFT) methods of calculations in the analysis of vibrational frequency, charge distributions, and magnetic resonance parameters for indol-3- and indazole-3-carboxylate derivatives of cannabinoids (Table 1) and the calculated results are correlated to the experimental data. The application of theoretical tools, makes these tasks easier and attainable. Especially when the results obtained from theoretical studies are in good agreement with the reported empirical data.

Methods

Computational details

The equilibrium geometries of a series of indol-3-carboxylate and indazole-3-carboxylate derivatives of cannabinoids consisting of five molecules were optimized at density functional theory (DFT) methods. The DFT/B3LYP/6-311G** was used to calculate and investigate the unscaled vibrational frequency and chemical shifts of the modeled molecules. The convergence criteria for the energy calculations and geometry optimizations used in the density functional methods were default parameters in the Spartan' 14 program implemented on an Intel® Core(TM) i5-5200U CPU @ 2.20GHz, 8G RAM Dell computer. The E_{HOMO} and E_{LUMO} of the modeled molecules are related to the ionization potential (IP) and the electron affinity (EA), respectively using Koopman's theorem (Pearson, 1986) by the following relationships:

$$I = -E_{HOMO} \qquad (1)$$
$$A = -E_{LUMO} \qquad (2)$$

The electronegativity, χ, and the hardness, η, of the inhibiting molecule are given as (Parr and Pearson 1983):

$$\chi = -\mu = \left(\frac{\delta\varepsilon}{\delta N}\right)_{v(r)} = -\frac{E_{LUMO} + E_{HOMO}}{2} = \frac{IP + EA}{2} \qquad (3)$$

$$\eta = \left(\frac{\delta\varepsilon^2}{\delta N^2}\right)_{v(r)} = \frac{E_{LUMO} + E_{HOMO}}{2} = \frac{IP - EA}{2} \qquad (4)$$

Furthermore, softness is defined as the inverse of the hardness value (Chirico and Gramatica, 2012):

$$\sigma = \frac{1}{\eta}$$

The electrophilic index is calculated using

$$\omega = \frac{\mu^2}{2\eta} \qquad 3.3$$

Results

Modeled and optimized structures.

The conventional names, molecular formula, and preferable chemical names or synonyms of the synthetic cannabinoids are presented in Table 1 while the labeled molecular structure (left hand side) and optimized structures of five synthetic medical cannabinoids studied are presented as Figure 1. The molecular formulae of the modeled compounds: $C_9H_{26}FN_3O_3$, $C_{20}H_{28}FN_3O_3$, $C_{21}H_{22}FN_3O_3$, $C_{22}H_{24}FN_3O_3$ and $C_{22}H_{31}N_3O_3$, are represented by M1, M2, M3, M4 and M5 respectively. In the modelled compounds there are two indole (M1- M2) and three indazole (M3 – M5) based groups. Figure 1 clearly shows the structural differences of the two indoles and the three indazoles. For instance, M1 has linear chain attached to the N- (indole) with naphthalene to the O of the carboxylate while phenyl fluoride and quinolin are found in M2. The implication is that the two compounds are indole-3-carboxylates but due to structure differences they are bound to have different chemical reactivities and spectrophotometric information. On the hand, the three indazole (M3 – M5) known as indazole-3-carboxylates are characterized with two nitrogen atoms (as against one in the indole-3-carboxylates). The three molecules also have noticeable structural differences; M3 has quinolin and phenyl fluoride, M4 has quinolin and pentyl fluoride and M5 has naphthalene and phenyl fluoride. These compounds may have similar application(s) but their chemical reactivities would be different.

In the optimized structures colour codes as available on the modeled structures to that mean that the gray balls are carbon (C) atoms, the red ones represent oxygen (O) atoms, the white balls denote hydrogen (H) atoms, yellow balls are fluorine (F) atoms and the blue balls mean nitrogen (N) atoms.

Table 1: Structures and Chemical Names of Compounds M1 – M5

Compound	Conventional name	Molecular structure	Chemical name
M1	CBL-2201 (NM-2201)		Naphthalene-1-yl 1-(5-fluoropentyl 1H-indole-3-carboxylate)
M2	QCBL-Bz-F(FUB-PB-22; MN-27)		Quinolin-8-yl 1-(4-fluorobenzyl 1H-indole-3-carboxylate)
M3	QCBL(N)-Bz-F(FUB-NPB-22)		Quinolin-8-yl 1-(5-fluoropentyl)-1H-indazole-3-carboxylate
M4	QCBL(N)-2201(5-fluoro NPB-22		Quinolin-8-yl 1-(5-fluoropentyl)-1H-indazole-3-carboxylate
M5	CBL(N)-2201(5-fluoro SDB-005)		Naphthalen-1-yl 1-(5-fluoropentyl)- 1H-indazole-3-carboxylate

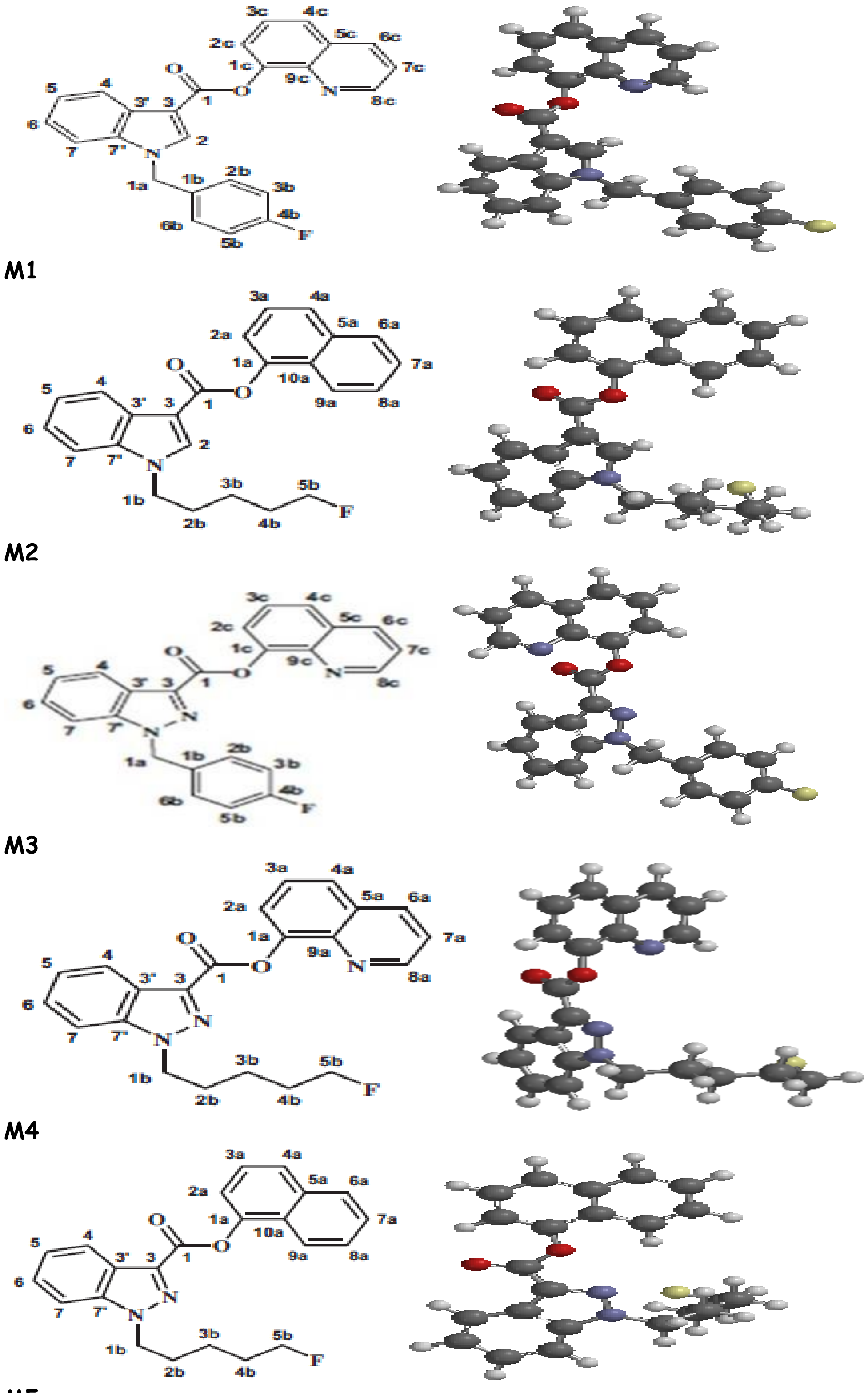

Figure 1: Labeled optimized structures of the studied cannabinoids at DFT/B3LYP level. Colour codes for the atoms in the molecules: H=white; O=red; N=blue ball; C=ash; F=Yellow

Frontier molecular orbitals and global reactivity descriptors

With reference to the information presented as Figure 2 and Table 2, the highest occupied molecular orbital energy (HOMO) and lowest unoccupied molecular orbital energy (LUMO) are referred to as the frontier molecular orbitals. The frontier molecular orbital energies are used to determine the way a molecule interacts with other species. The HOMO is the orbital energy that donates electron, since it is the outermost (highest energy) orbital containing electrons. The LUMO is the orbital that accepts electron, since it is the innermost (lowest energy) orbital that has capability of accepting electrons (Raja *et al.,* 2015). According to the frontier molecular orbital theory, a transition state is formed due to an interaction between the frontier orbitals (HOMO and LUMO) of reactants. The energy of the HOMO is directly related to the ionization potential (IP) and the energy of the LUMO is directly related to the electron affinity (EA). The HOMO–LUMO gap (E_g), i.e. the difference in energy between the HOMO and LUMO, is also known as the band gap and is also an important parameter.

Highest energy band gap recorded for M3 is the highest compared with other molecules. It was noticed also that M5 has the lowest band gap with the value (4.11 eV). The band gap (E_g) indicates the stability for the molecule in chemical reactions (Kumara *et al.*, 2013). The values of the band gap follows: M3> M2> M4> M1> M5. It can therefore be predicted that M3 has the highest stability while M5 has the lowest stability and hence the highest conductivity. The electric dipole moment is the most extensively used quantity to describe the polarity of a molecule (Kumara *et al.*, 2013). It measures the degree of polarity of a polar covalent bond and can be defined as the product of charge on the atoms and the distance between the two bonded atoms. M2 has the highest value of dipole moment with 6.30 Debye followed by M5 (5.22 Debye). The results of the dipole moment shows that the degree of polarity is not centered on the attached moiety, the reason adducible to this lies in the fact that M2 and M5 has contrasting attachments or moieties. Chemical potential (*μ*) and chemical hardness (*η)* were estimated from the LUMO and HOMO data of the modeled compounds. These two parametersmeasure the tendency of an electronto escape from a particular field (Hazekamp *et al.,* 2013) and the resistance to modification of the electronic density respectively (Semire and Adeoye, 2013). The low values of *μ* for M3 (-3.97) and *η for* M5 (2.055) indicate that the molecules have more resistance to donating electron and that their electronic densities can be easily modifiedcompared to other modeled molecules. Chemical softness (*S*) gives relevant information about the chemical reactivity of a molecule. High value of softness relates to high chemical reactivity. From the data obtained for the chemical softness of the modeled compounds, M1 (*0.235*) has the highest *S* value followed by M5 (*please write the value for M5*).

The electrophilicity index (ω) of the molecules calculated showed that M2 has the lowest value (2.745) and it is an indication that it has the lowest capability to accept electron (Semire and Adeoye, 2013) compared to other modeled compounds.

Table 2: Global Reactivity Descriptors of the Cannabinoids

Compounds	HOMO	LUMO	E_g	DM	η	*μ*	*S*	ω
M1	-5.92	-1.66	4.26	3.16	2.130	-3.790	0.235	3.370
M2	-5.80	-1.26	4.54	6.30	2.270	-3.530	0.220	2.745
M3	-6.26	-1.68	4.58	2.04	2.290	-3.970	0.218	3.441
M4	-6.14	-1.61	4.53	3.39	2.265	-3.875	0.221	3.315
M5	-5.79	-1.68	4.11	5.22	2.055	-3.735	0.243	3.394

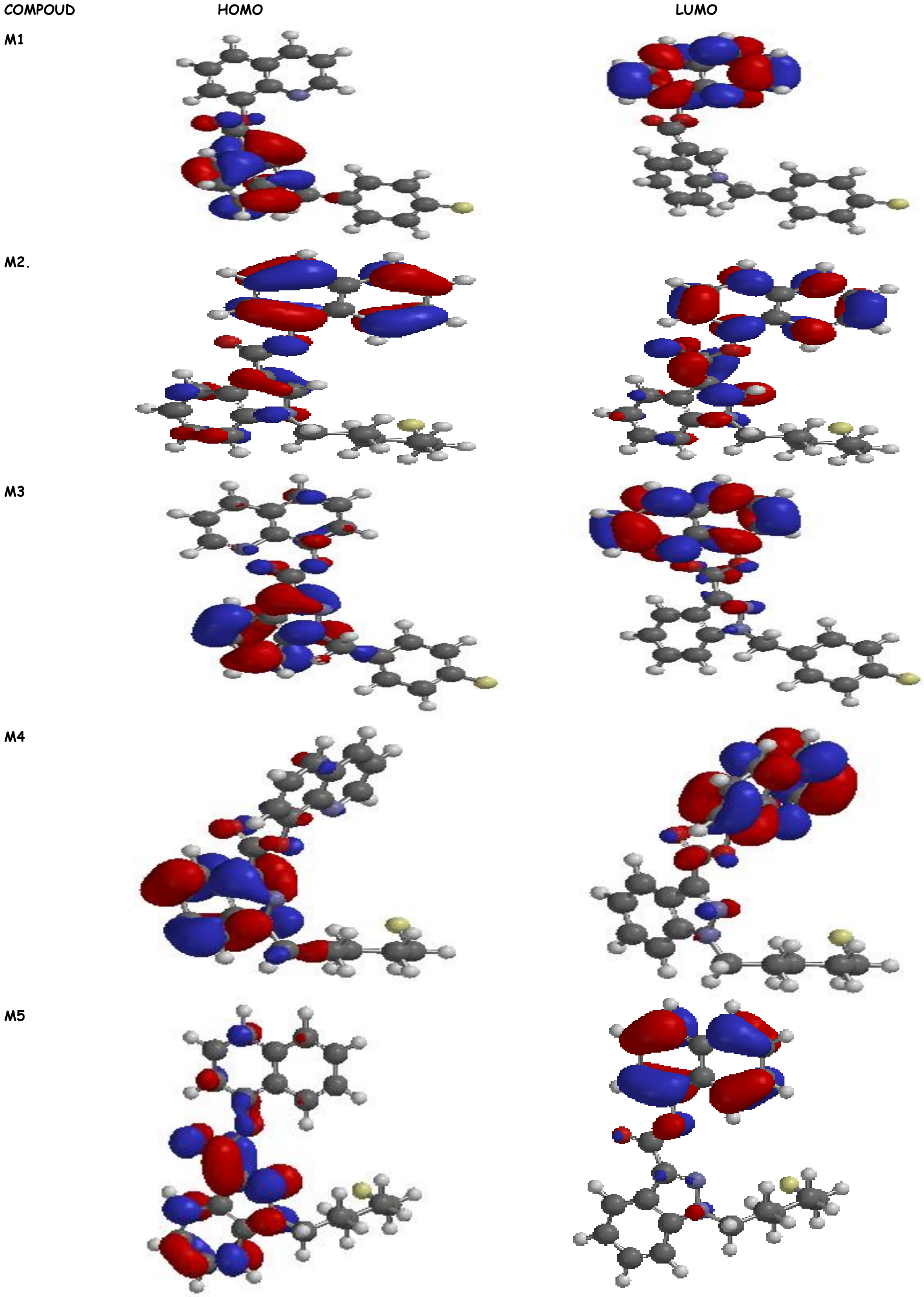

Figure 2: Frontier molecular orbital overlays of the molecules (M1 – M5).

Chemical Shifts

Nuclear magnetic resonance (NMR) permits the observation of specific quantum mechanical property of the atomic nucleus. The optimized structures of the studied molecules at DFT method with 6-311G* basis set were used to calculate chemical shift for the molecules and the data obtained are presented as Tables 3 – 7. Correlation diagram (graph) Figure 3 were used to interpret the data comparison. From these Tables and Figures, it was observed that ^{13}C and ^{1}H NMR calculated using DFT were in good agreement with the experimental (Shafran *et al.*, 2014). It was also observed from the tables that the values of ^{13}CNMR obtained are relatively above 100 ppm which is a typical chemical shift for aromatics (Stare *et al*, 2004). These data can be attributed to the fact that the carbon nuclei are affected by electronegativity of π- donors. The effect of this is that the chemical shift of the carbon atom increases as the π-donors become more electronegative. For instance in the case of M1 some of the highest chemical shifts of ^{13}C are 152.973 (C8c), 166.792 (M1) and 171.926 ppm (M4b) for B3LYP/6-311G*, it can be deduced that the presence ofnitrogen, oxygen and fluorine attached to these carbon atoms pulls a great electronegativity effect on them, therefore (M4b) experienced more de-shielding effect than all other carbon atoms due to higher electronegativity effect of fluorine. For M1 (^{1}HNMR values for carbon atoms), the empirical data were in good agreement with the theoretical. The observed variations (as observed that the empirical data were higher than the theoretical) can be attributed to the facts that the compounds are not in the same medium (theoretical calculations were performed in gas phase) and the effect of hyperfine structures upon which the theoretical calculations were carried out. All these bring about the difference in the quantity of the data obtained for the empirical and theoretical studies. For the ^{13}C values, comparison between the experimental and theoretical chemical shifts (^{13}C) of the studied compounds was explained with graph (Figure 3) based on the available data presented as Table 3. For M2, the ^{1}HNMR and ^{13}C values were calculated and comparison was drawn with experimental using correlation diagram (Figure 3). Also the experimental chemical shifts are compared with the theoretical calculated values using ab initio and DFT methods as listed in Table 4. Table 5 provide the data for M3 ^{1}HNMR values for C1a, C2c, C6c, C7c and C8c are calculated at DFT, experimental data and comparison between the experimental and theoretical chemical shifts (^{13}C) of the studied compound presented as Figure 3.

Similarly, as explained above, for M4, the ^{1}HNMR and ^{13}CNMR values for C2a, C4a, C6a, C7a and C8a are calculated using DFT/B3LYP method. Comparison between the experimental and theoretical chemical shifts (^{13}C) is presented in Figure 3. Also the experimental chemical shifts are compared with the theoretical calculated values using DFT/B3LYP methods as shown in Table 5. For M5, the ^{1}HNMR ^{13}C-NMR values for C4, C1b, C2b, C3b and C4b were calculated using the quantum mechanical method and correlation with experimental is shown in Figure 3. It was observed from the graph thatM4 has the best chemical shift correlation values (0.9956) for DFT/B3LYP.

Table 3: Empirical and Theoretical Chemical Shifts for using B3LYP/6-311 Method.

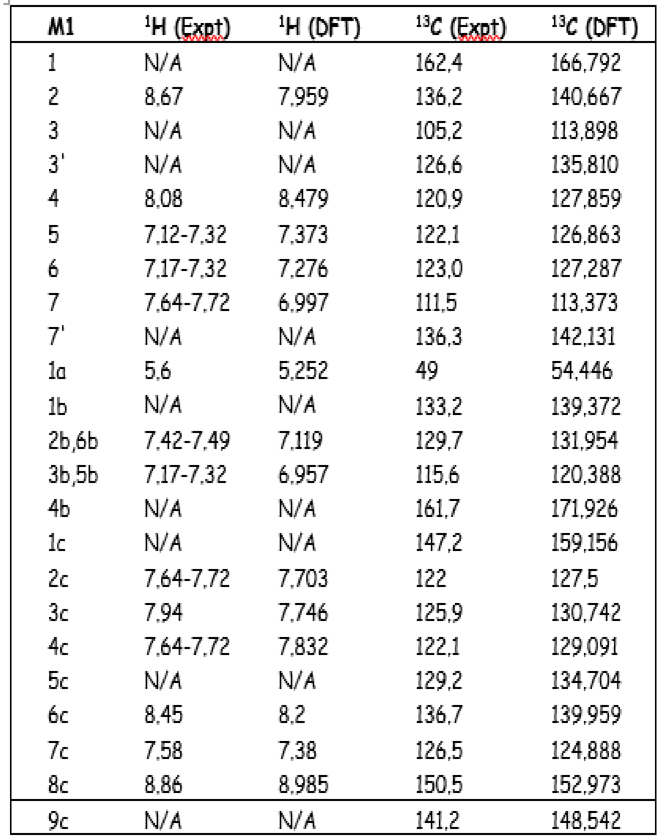

M1	^{1}H (Expt)	^{1}H (DFT)	^{13}C (Expt)	^{13}C (DFT)
1	N/A	N/A	162,4	166,792
2	8,67	7,959	136,2	140,667
3	N/A	N/A	105,2	113,898
3'	N/A	N/A	126,6	135,810
4	8,08	8,479	120,9	127,859
5	7,12-7,32	7,373	122,1	126,863
6	7,17-7,32	7,276	123,0	127,287
7	7,64-7,72	6,997	111,5	113,373
7'	N/A	N/A	136,3	142,131
1a	5,6	5,252	49	54,446
1b	N/A	N/A	133,2	139,372
2b,6b	7,42-7,49	7,119	129,7	131,954
3b,5b	7,17-7,32	6,957	115,6	120,388
4b	N/A	N/A	161,7	171,926
1c	N/A	N/A	147,2	159,156
2c	7,64-7,72	7,703	122	127,5
3c	7,94	7,746	125,9	130,742
4c	7,64-7,72	7,832	122,1	129,091
5c	N/A	N/A	129,2	134,704
6c	8,45	8,2	136,7	139,959
7c	7,58	7,38	126,5	124,888
8c	8,86	8,985	150,5	152,973
9c	N/A	N/A	141,2	148,542

Note: N/A= not applicable.

Table 4: Empirical and Theoretical Chemical Shifts For M2 Using B3LYP/6-311G Methods.**

M2	^{1}H (Expt)	^{1}H (DFT)	^{13}C (Expt)	^{13}C (DFT)
1	N/A	N/A	162,5	165,898
2	8,6	7,94	136,9	136,572
3	N/A	N/A	104	114,591
3'	N/A	N/A	127	134,453
4	8,07	8,61	120,6	128,132
5	7,25-7,31	7,443	122,1	126,946
6	7,31-7,36	7,435	122,8	127,505
7	7,72	7,228	111,3	111,643
7'	N/A	N/A	136,6	144,21
1a	N/A	N/A	146,4	154,166
2a	7,45	7,615	118,9	124,563
3a	7,52-7,63	7,655	126,4	129,623
4a	8,03	7,78	128	128,803
5a	N/A	N/A	134,2	140,246
6a	7,87-7,91	7,937	125,6	132,381
7a	7,52-7,63	7,613	126,5	130,138
8a	7,52-7,63	7,608	126,6	129,605
9a	7,90-7,94	8,352	121,2	126,71
10a	N/A	N/A	125,8	133,284
1b	4,34-4,42	4,187	46,2	48,569
2b	1,91	1,951	29,1	37,425
3b	1,4	1,435	22	27,649
4b	1,63-1,78	1,564	29,3	36,319
5b	4,34-4,42	4,502	83,7	86,337

Note: N/A= not applicable.

Table 5: Empirical And Theoretical Chemical Shifts For M3 Using B3LYP/6-311G Methods**

M3	^{1}H (Expt)	^{1}H (DFT)	^{13}C (Expt)	^{13}C (DFT)
1	N/A	N/A	160,8	166,334
3	N/A	N/A	134,2	140,981
3'	N/A	N/A	127,8	132,803
4	8,18	8,541	121,9	128,721
5	7,16-7,25	7,384	124	127,192
6	7,16-7,25	7,432	124,2	130,549
7	7,97-8,02	7,312	111,6	112,111
7'	N/A	N/A	141	146,083
1a	5,89	5,507	52,6	57,581
1b	N/A	N/A	133,2	139,193
2b,6b	7,54-7,59	7,561	130,4	134,404
3b,5b	7,37-7,48	6,956	116,1	120,09
4b	N/A	N/A	162,3	172,174
1c	N/A	N/A	147,2	159,035
2c	7,77	7,762	122,3	126,582
3c	7,97-8,02	7,761	126,9	130,721
4c	7,67-7,74	7,835	122,7	129,129
5c	N/A	N/A	129,7	134,676
6c	8,49	8,199	136,8	139,878
7c	7,61	7,378	127	124,918
8c	8,86	8,946	151,2	152,884
9c	N/A	N/A	141	147,639

Note: N/A= not applicable.

Table 6: Empirical and Theoretical Chemical Shifts Of M4 Using B3LYP/6-311G Methods.**

M4	^{1}H (Expt)	^{1}H (DFT)	^{13}C (Expt)	^{13}C (DFT)
1	N/A	N/A	160,4	166,068
3	N/A	N/A	133,0	141,47
3'	N/A	N/A	123,3	131,711
4	8,17	8,559	121,3	128,828
5	7,35-7,43	7,404	123,6	126,876
6	7,52-7,58	7,507	126,9	130,454
7	7,94	7,318	111,0	111,049
7'	N/A	N/A	140,6	148,068
1a	N/A	N/A	146,8	158,994
2a	7,78	7,734	121,9	126,496
3a	7,67-7,74	7,723	126,5	130,598
4a	7,99	7,788	126,3	129,025
5a	N/A	N/A	129,2	134,583
6a	8,48	8,149	136,3	139,711
7a	7,6	7,344	122,2	124,827
8a	8,87	8,968	150,7	153,038
9a	N/A	N/A	140,6	147,827
1b	4,64	4,369	49,2	52,269
2b	1,98	2,158	29,0	35,612
3b	1,4	1,452	22,1	28,834
4b	1,62-1,78	1,525	29,3	36,232
5b	4,36 and 4,48	4,517	83,6	86,988

Note: N/A= not applicable.

Table 7: Empirical And Theoretical Chemical Shifts For M5 Using B3LYP/6-311G Methods**

M5	^{1}H (Expt)	^{1}H (DFT)	^{13}C (HF)	^{13}C (DFT)
1	N/A	N/A	162,413	165,008
3	N/A	N/A	140,943	141,727
3'	N/A	N/A	123,958	131,598
4	8,18	8,793	131,494	128,879
5	7,39-7,45	7,518	111,928	127,545
6	7,52-7,65	7,569	135,696	130,929
7	7,89-7,98	7,356	111,133	111,357
7'	N/A	N/A	149,656	148,051
1a	N/A	N/A	149,938	156,821
2a	7,52-7,65	9,159	123,674	118,43
3a	7,52-7,65	7,621	130,126	130,309
4a	8,03-8,08	7,697	129,573	128,394
5a	N/A	N/A	140,942	139,937
6a	7,89-7,98	7,86	131,926	131,744
7a	7,52-7,65	7,624	131,275	130,333
8a	7,52-7,65	7,705	130,128	129,435
9a	7,89-7,98	9,131	128,221	128,221
10a	N/A	N/A	133,784	131,806
1b	4,66	4,372	46,208	51,624
2b	1,99	2,489	30,702	33,727
3b	1,41	1,44	23,432	27,806
4b	1,62-1,78	1,641	30,891	36,084
5b	4,36 and 4,48	4,496	74,513	86,735

Note: N/A= not applicable.

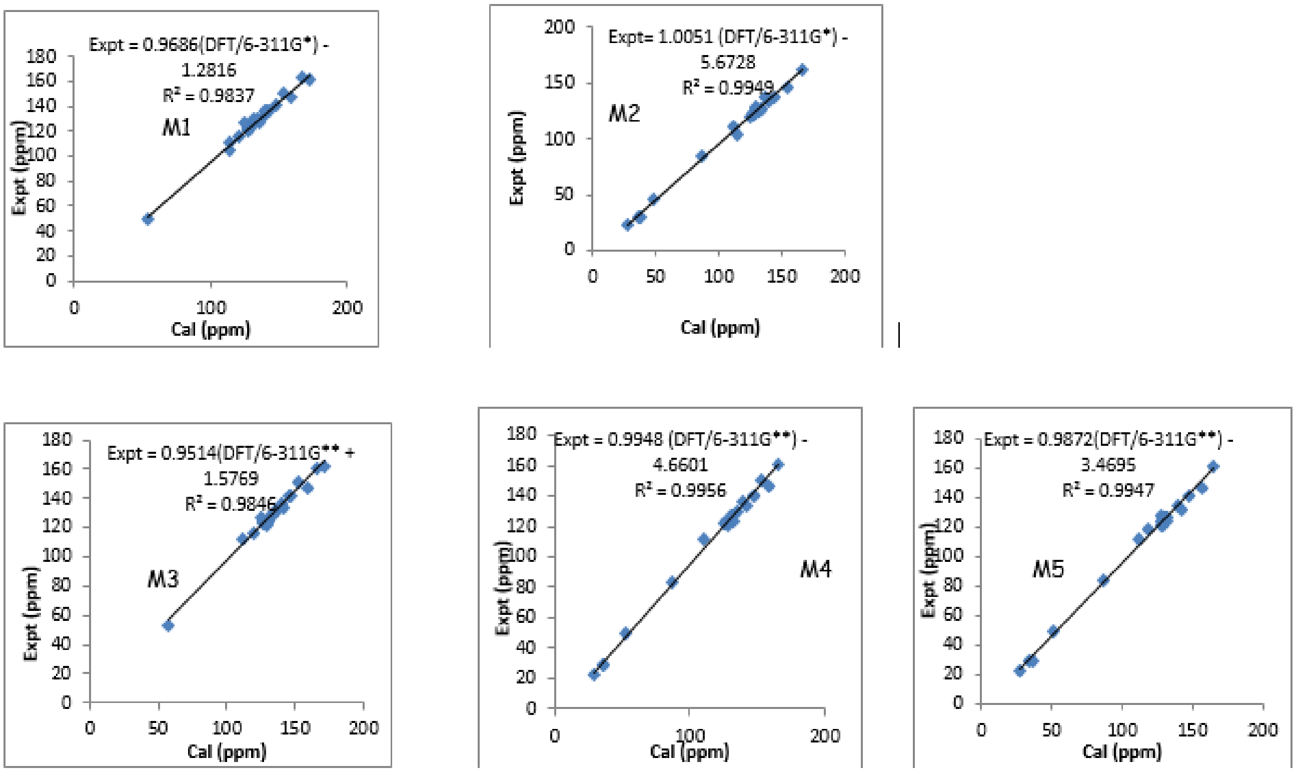

Figure 3: Graphs showing the correlation between empirical and theoretical chemical shifts for molecules using DFT/6-311G**

Vibrational Frequencies

One of the methods used in organic chemistry to identify functional groups of organic compounds and also to distinguish molecular conformers as well as isomers is vibrational spectroscopy. In order to obtain the spectroscopic signature of the study molecules frequency calculation analysis was performed and vibrational frequencies are calculated using B3LYP/6-311G**.The vibrational frequencies calculated at B3LYP/6-311G** level for the five molecules are shown in Tables 7, 8 and 9. All the theoretical calculation are compared to the experimental values by Shafran, et al 2015. These tables present a good tendency to easy comparison between the experimental and calculated vibrational frequencies. One of the methods used in organic chemistry to identify functional groups of organic compounds and also to distinguish molecular conformers as well as isomers is vibrational spectroscopy. In order to obtain the spectroscopic signature of the study molecules frequency calculation analysis was performed and vibrational frequencies are calculated using B3LYP/6-311G**.The vibrational frequencies calculated at B3LYP/6-311G** level for the five molecules are presented as Tables 4.8 – 4.10. All the theoretical calculation are compared to the experimental values by Shafran *et al.*, .These tables present a good tendency to easy comparison between the experimental and calculated vibrational frequencies.

C-H Vibration

The heteroatomic structure shows that the presence of C-H stretching vibration is in the region 3100-3000cm^{-1} which is the characteristic region for the ready identification of C-H vibration (Kumara *et al.*, 2013). The calculated bands are 3262-3143, 3262-3113, 3221-3145, 3220-3146 and 3260-3160 cm^{-1} for M1, M2, M3, M4 and M5 respectively at DFT/6-311G**. The empirical bands observed at 3122.5, 3132, 2924.1, 3065.1 and 3062 cm^{-1} for M1, M2, M3, M4 and M5 are assigned to C-H stretching vibration. The aromatic C-H in-plane bending vibration occur in the region 1300-1000cm^{-}

^{1}, the bands are sharp but have weak to medium intensities. The C-H in-plane bending vibration computed at 1162-1049cm^{-1} shows good agreement with FT-IR band at 1174.7 for M1. The bands observed at 989.5-750.3 experimentally are assigned to C-H out of plane bending for the study molecules. This also shows good agreement with the theoretically studied values.

C-C Vibration

The ring stretching vibrations are very prominent as the double bond is in conjugation with the ring in the vibrational spectra of benzene and its derivatives. The bands were observed experimentally at 1376.8, 1461.1, 1441.1, 1398.3 and 1386.2cm^{-1} M1 – M5 respectively. The theoretically computed values at 1466, 1492-1440, 1433, 1421 and 1388cm^{-1} respectively shows a good agreement with the experimental data.

C=O vibration

The carbonyl group is important and its characteristic frequency has been extensively used to study a wide range of compounds. If a compound contains a carbonyl group, the absorption caused by C=O stretching is generally, the strongest present (Hassan, 2010). The C=O stretching frequency appears strongly in the infrared spectrum in the range 1600-1850cm^{-1}. The experimental vibrational frequencies were 1722, 1707.2, 1723.2, 1731.2 and 1730cm^{-1} for M1 – M5 respectively, DFT calculation give C=O stretching mode at 1801, 1790, 1797, 1795 and 1768 cm^{-1}

C-N and C=N Vibrations

The medium to weak bands for the C-N linkages in amines appear in the region 1200-1020cm^{-1}. The ring C=C and C=N stretching vibration occur in the region 1615-1573cm^{-1} and 1520-1465 cm^{-1} . The C-N stretching vibration is observed in the region 1378.6, 1461.1, 1411.1, 1414.7 and 1386.2cm^{-1} for M1 – M5 respectively. DFT calculation gives the stretching vibrations at 1405, 1492-1440, 1408, 1418 and 1388cm^{-1} M1 – M5 respectively. C=N stretching vibration is observed at 1508.6, 1510.1, 1467.4 and 1466.5 cm^{-1} for M1, M3, M4 and M5. DFT calculation give C=N stretching at 1508, 1665-1506, 1452 and 1466cm^{-1}. In general, the C=N vibrations computed by B3LYP/6-311G** show good agreement with empirically observed data.

C-F, C-O and N-N Vibrations

The C-F vibrations give generally strong bands in the region 1000-1400 cm^{-1}.Although these bands are not observed experimentally but DFT calculations gave C-F vibrations at 1261, 1060, 1260, 1058 and 1089cm^{-1} for M1 - M5 respectively. The bands observed at 1314.4, 1313.7 and 1105.2cm^{-1} for M3, M4 and M5 experimentally are attributed to N-N stretching vibrations of the molecules. The theoretical calculations by B3LYP method has provisions for the vibrations at 1327,1313 and 1113cm^{-1} for M3, M4 and M5 exactly corresponding with experimental findings. The C-O stretching of the aromatic ring in IR spectrum is characterized by the frequency around 1270-1230cm^{-1}. The experimental vibrational frequency is observed at 1240.6, 1201.9, 1162.7 and 1223.6 cm^{-1} for M1, M2, M4 and M5. The theoretical frequency around 1267, 1220, 1245 and 1224 respectively, corresponds satisfactorily with the experimental data. In addition, the spectra of the experimental and simulated IR frequencies using DFT/6-311G** are presented as Figure 4

Table 8: Selected Theoretical (B3LYP/6-311G) and Empirical Vibrational Frequencies for Molecule M1**

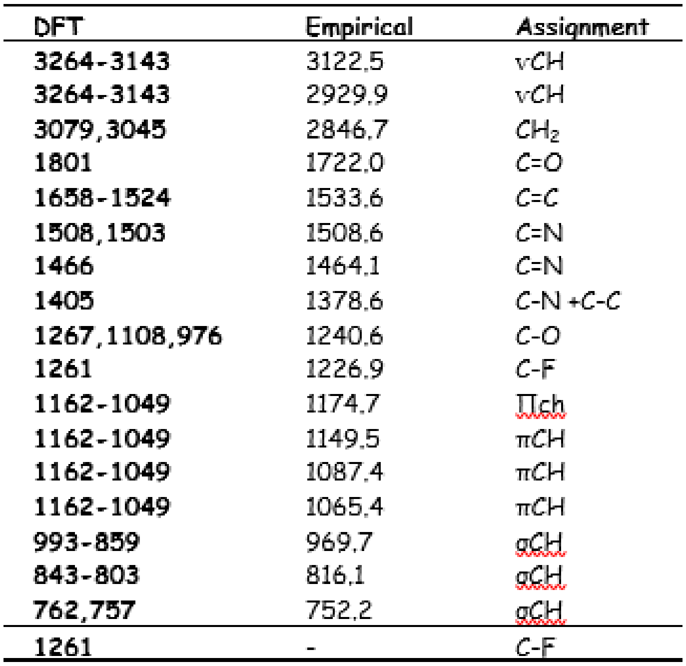

DFT	Empirical	Assignment
3264-3143	3122.5	vCH
3264-3143	2929.9	vCH
3079,3045	2846.7	CH_2
1801	1722.0	C=O
1658-1524	1533.6	C=C
1508,1503	1508.6	C=N
1466	1464.1	C=N
1405	1378.6	C-N +C-C
1267,1108,976	1240.6	C-O
1261	1226.9	C-F
1162-1049	1174.7	∏ch
1162-1049	1149.5	πCH
1162-1049	1087.4	πCH
1162-1049	1065.4	πCH
993-859	969.7	αCH
843-803	816.1	αCH
762,757	752.2	αCH
1261	-	C-F

Table 9: Selected Theoretical (B3LYP/6-311G) and Empirical Vibrational Frequencies for Molecules M2 and M3**

		M2			M3
DFT	**Experimental**	**Assignment**	**DFT**	**Experimental**	**Assignment**
3262-3113	3132.2	νCH	**3269-3160**	3062.0	νCH
3262-3113	3060.4	νCH	**3111-3009**	2957.6	νCH_2
3092-3011	2961.5	νCH_2	**1768**	1738.8	C=O
1790	1707.2	C=O	**1449**	1466.5	C=N
1674-1551	1531.9	C=C	**1388**	1386.2	C-C
1492-1440	1461.1	C=C + CH_2+C-N	**1224**	1223.6	C-O
1220,1197,978	1201	C-O	**1141**	1152.1	CO
1105,1088	1139.1	C-O	**1113**	1105.2	N-N +C-O +CH
1105,1088	1091.0	C-O	**990-915**	985.8	σCH
982-798	969.7	σCH_2	**788,768**	789.9	σCH
982-798	868.1	σCH_2	**788,768**	767.9	σCH
1060,1080		C-C + C-F	**1089,1049**		C-F + C-C

Table 10: Some Selected Theoretical (B3LYP/6-311G) and Experimental Vibrational Frequencies For Molecules M3 and M4.**

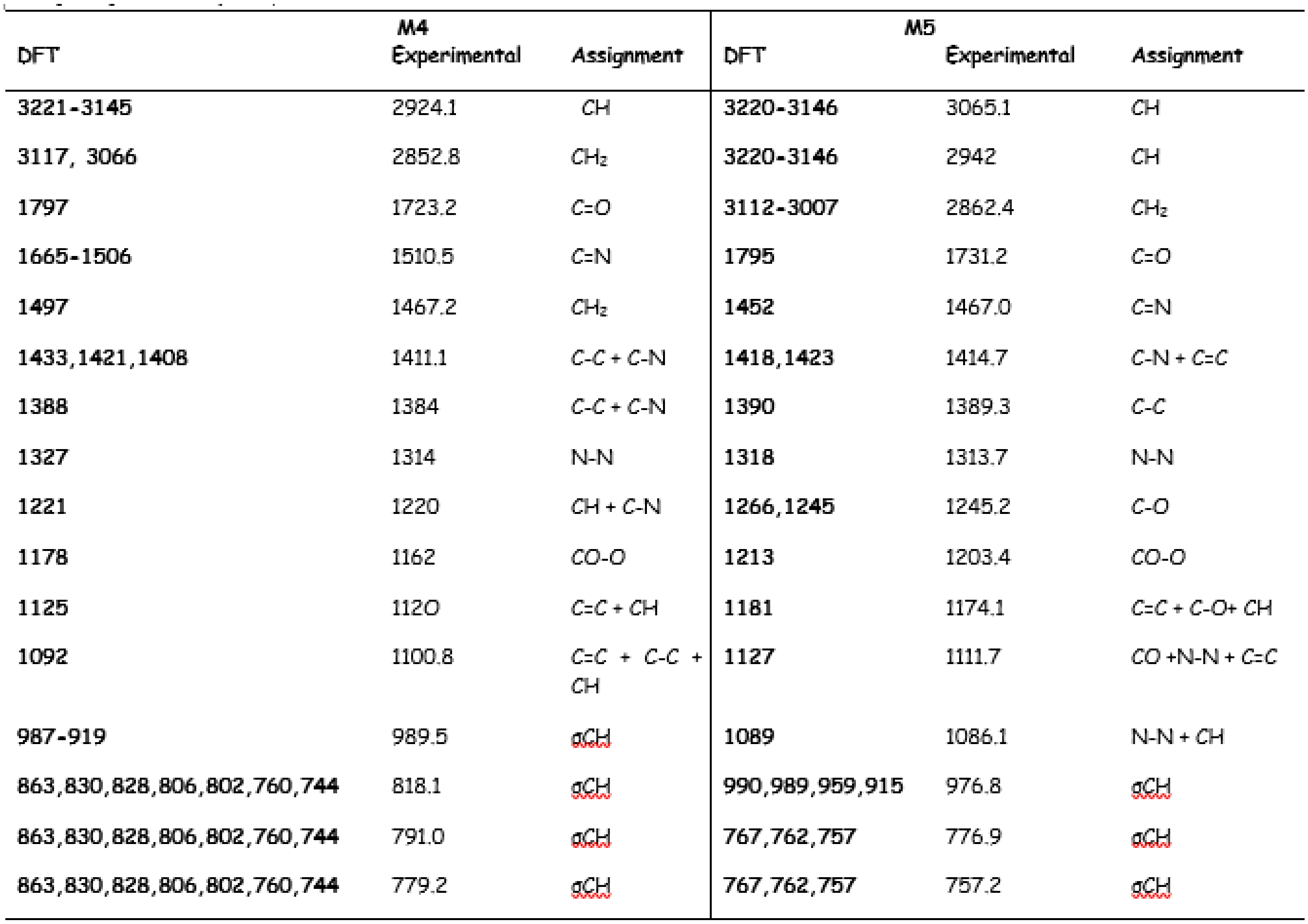

	M4			M5	
DFT	Experimental	Assignment	DFT	Experimental	Assignment
3221-3145	2924.1	CH	3220-3146	3065.1	CH
3117, 3066	2852.8	CH_2	3220-3146	2942	CH
1797	1723.2	C=O	3112-3007	2862.4	CH_2
1665-1506	1510.5	C=N	1795	1731.2	C=O
1497	1467.2	CH_2	1452	1467.0	C=N
1433,1421,1408	1411.1	C-C + C-N	1418,1423	1414.7	C-N + C=C
1388	1384	C-C + C-N	1390	1389.3	C-C
1327	1314	N-N	1318	1313.7	N-N
1221	1220	CH + C-N	1266,1245	1245.2	C-O
1178	1162	CO-O	1213	1203.4	CO-O
1125	1120	C=C + CH	1181	1174.1	C=C + C-O+ CH
1092	1100.8	C=C + C-C + CH	1127	1111.7	CO +N-N + C=C
987-919	989.5	σCH	1089	1086.1	N-N + CH
863,830,828,806,802,760,744	818.1	σCH	990,989,959,915	976.8	σCH
863,830,828,806,802,760,744	791.0	σCH	767,762,757	776.9	σCH
863,830,828,806,802,760,744	779.2	σCH	767,762,757	757.2	σCH

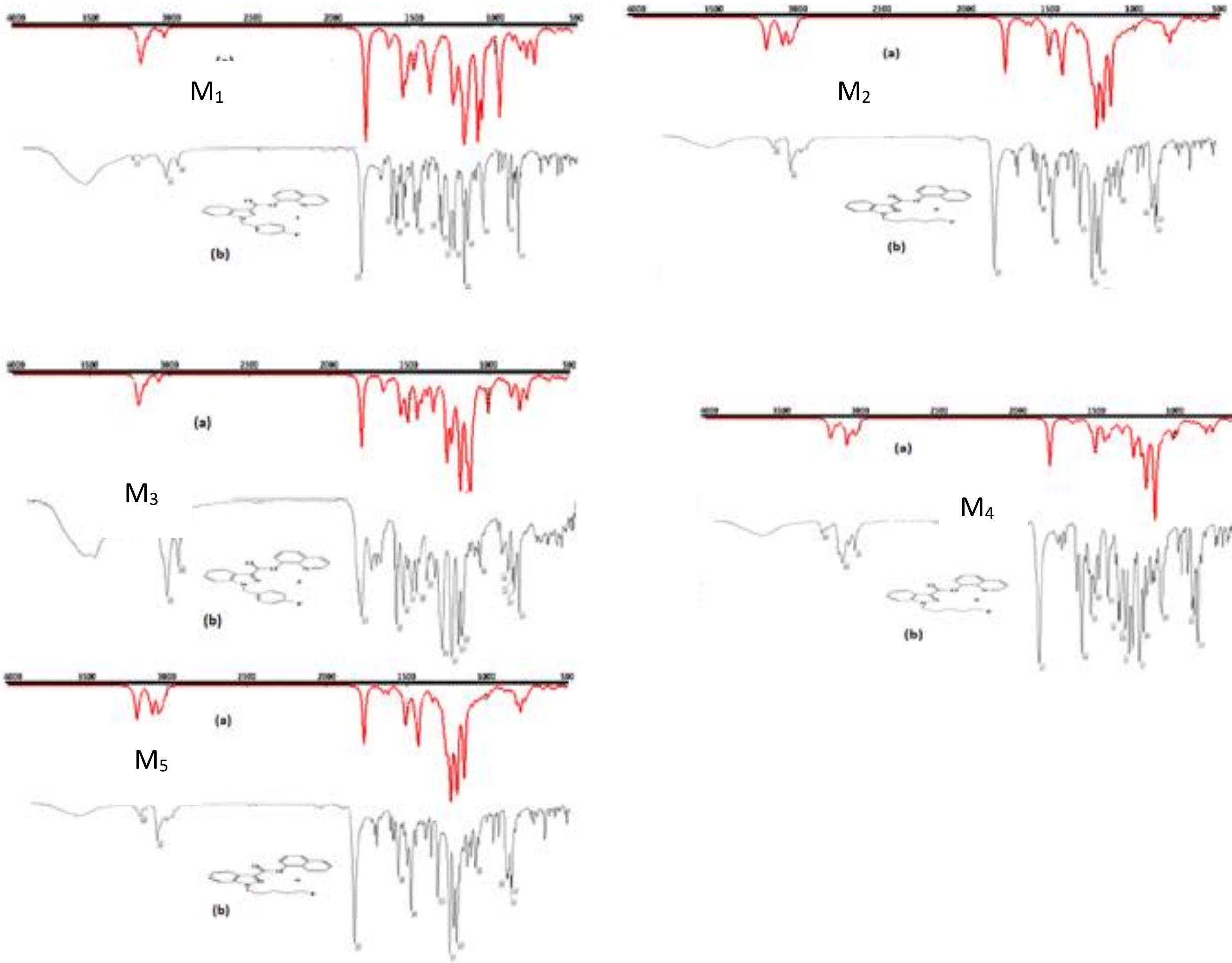

Figure 4: IR spectra for M1-M5; (a) Simulated (DFT/6-311G) and (b) Experimenta**

Conclusion

In this work, computational approach has been used to study the spectroscopic properties of synthetic five cannabinoids at DFT/B3LYP/6-311G** and the theoretical results obtained compare favourably with the empirical data earlier reported. The electronic properties, global reactivity indices and spectroscopic properties of the molecules were studied. The energy band gaps calculated showed that Naphthalene-1-yl 1–(5-fluoropentyl)-1H-indazole-3-carboxylate (M5) has the lowest band gap energy indicating its substantial influence on the intramolecular charge transfer. The vibrational frequency analyses by DFT/B3LYP method are in reasonable agreement with the experimental values. The ^{13}C and ^{1}HNMR chemical shifts calculated at DFT agreed with the experimental data. DFT/6-311G** has the best correlation with fitting factor 0.9956.Thus the chemical shifts from DFT/6-311G** are accurate and can be used in the absence of experimental data. The frequencies, MOs and λ_{max} of the compounds were also evaluated from DFT method.

References

Belendiuk, K. A., Baldini, L. L., & Bonn-Miller, M. O. (2015). Narrative review of the safety and efficacy of cannabis for the treatment of commonly state-approved medical and psychiatric disorders. *Addictive Science Clinical Practise*. 21; 10(1): 10.

Eisenberg, E., Ogintz, M., & Almog, S. (2014). The pharmacokinetics, efficacy, safety, and ease of use of a novel portable metered-dose cannabis inhaler in patients with chronic neuropathic pain: a phase 1a study. Journal of Pain Palliative Care Pharmacother. 28(3): 216-25.

Ellis, R. J., Toperoff, W., Vaida, F., Van den Brande, G., Gonzales, J., Gouaux, B., Bentley, H., &

Atkinson, J. H. (2009). Smoked medicinal cannabis for neuropathic pain in HIV: a randomized, crossover clinical trial. *Neuro-psycho Pharmacology*. 34(3): 672-80.

Hassan, T. (2010). Quantum chemical computational studies on 2-methyl-6-[2-(trifluoromethyl) phenyl iminomethyl] phenol. *Journal of Molecular Structure*: *Theoretical Chemistry*. 950: 5-12

Hazekamp, A., Ware, M. A., Muller-Vahl, K. R., Abrams, D., & Grotenhermen, F. (2013). The medicinal use of cannabis and cannabinoids—an international cross-sectional survey on administration forms. *Journal of Psychoactive Drugs* 45, 199-210.

Jorge, F. E., Morigaki, M. K., & Sara, S. J. (2012) Quantum Chemical Investigation on determination of electronic, structural and electrical properties of some even carbon cage fullerenes, Indian Journal of Chemistry 51, 911-916.

Kumara, N. T. R. N., Muhammad, R. R. K., Andery, L., Mohammad, I. P., Nyuk, Y. V., Chee, M. L., & Piyasiri E. (2013). DFT/TDDFT and Experimental Studies of Natural Pigments Extracted from Black Tea Waste for DSSC Application. *International Journal of Photoenergy*. 1-8.

Lundqvist, M. J., Nilsing, M., Persson, P., & S. Lunell. (2006). Spacer and anchor effects on the electronic coupling in Ruthenium bis-terpyridine dye-sensitized TiO_2 nanocrystals studied by DFT. *International Journal of Quantum Chemistry*. 106: 3214-3228.

Manhapra, A., Stefanovics, E., & Rosenheck, R. (2015). Treatment outcomes for veterans with PTSD and substance use: Impact of specific substances and achievement of abstinence. *Drug Alcohol Dependence*. (15) 01664-6.

Naftali, T., Bar-Lev, S. L., Dotan, I., Lansky, E. P., Sklerovsky B. F., & Konikoff F. M. (2013) Cannabis induces a clinical response in patients with Crohn's disease: a prospective placebo-.

Ono M., Ogilvie J. M., Wilson, J. S., Green, H. J., Chambers, S. K., Ownsworth, T., & Shum, D. H. (2015). A meta-analysis of cognitive impairment and decline associated with adjuvant chemotherapy in women with breast cancer. *Front Oncology*. 50-59.

Rajal, G, Saravanan, K., & Sivakumar, S. (2015). Quantum chemical and corrosion inhibition studies of an organic compound: 2, 5-dichloroaniline. *Rasayan Journal* 8(1), 8-12.

Semire, B., & Adeoye I. O. (2013). Molecular Orbital Studies (Hardness, Chemical Potential and Electrophilicity) and Solvent Effect on 3-Mehtyl-, 4-Methyl and 4-Phenylpicolinic Acid: Density Functional Theory (DFT). *Middle-East Journal of Scientific Research*, 18 (5), 597-608.

Shafran, Y., Vadim S., Vladimir, M., Alexander, N., Oleg, B., & Alexander B. (2014). Synthetic cannabinoids as designer drugs: New representatives of indol-3-carboxylates series and indazole-3-carboxylates as novel group of cannabinoids. Identification and analytical data, *Forensic Science International*, 244, 263–275.

Stern, E. & Lambert, D. M. (2007). Medicinal chemistry endeavors around the phyto-cannabinoids. *Chemical Biodiversity*: 4, 1707-1728.

Sun, X., Xu, C. S., Chadha, N., Chen, A., & Liu, J. (2015). Marijuana for Glaucoma: A Recipe for Disaster or Treatment? *Yale Journal Biological Medicine*. 88(3): 265-9.

Thomas, G., Kloner, R. A., & Rezkalla, S. (2014). Adverse cardiovascular, cerebrovascular, and peripheral vascular effects of marijuana inhalation: what cardiologists need to know? *American Journal of Cardiology*. 113(1): 187-90.

Ware, M. A., Wang, T., Shapiro, S., Robinson, A., Ducruet, T., Huynh, T., Gamsa, A., Bennett, G. J., & Collet, J. P. (2010). Smoked cannabis for chronic neuropathic pain: a randomized controlled trial. *Canadian Medical Association Journal*. 182(14): E694-701.

Wilkinson, S.T., Stefanovics, E., & Rosenheck, R. A. (2015). Marijuana use is associated with worse outcomes in symptom severity and violent behaviour in patients with posttraumatic stress disorder. *Journal of Clinical Psychiatry*. 76(9): 1174-80.